

Electrospun PLGA/multi-walled carbon nanotubes/wool keratin composite membranes: morphological, mechanical, and thermal properties, and their bioactivities in vitro

Hua-Lin Zhang · Juan Wang · Na Yu · Jin-Song Liu

Received: 6 September 2013 / Accepted: 26 November 2013 / Published online: 5 January 2014
© Springer Science+Business Media Dordrecht 2014

Abstract In this work, PLGA, multi-walled carbon nanotubes (MWNTs), and wool keratin were successfully electrospun to generate a series of PLGA/MWNTs/wool keratin membranes. The morphologies, structures, mechanical properties, thermal properties, and bioactivities of the resulting hybrid fibers were characterized using scanning electron microscopy (SEM), transmission electron microscopy (TEM), thermo-gravimetric analysis (TGA), tensile testing, and X-ray diffraction (XRD). The TEM results confirmed that the MWNTs and wool keratin particles were effectively incorporated into the composite fibers. The mechanical properties of the composites were significantly enhanced by the addition of the MWNTs. The PLGA/MWNTs/2.0 % wool keratin composite presented the best values of ultimate strength, elongation at break, and Young's modulus. All of the PLGA/MWNTs/wool keratin composites showed high thermal and thermooxidative stabilities. After mineralization, apatite crystals were deposited on the PLGA/MWNTs/wool keratin membranes, suggesting that the composites possess high bioactivity. Thus, these new ternary PLGA/MWNTs/wool keratin membranes show great potential to meet the demand for GBR membranes.

Keywords Multi-walled carbon nanotubes · Wool keratin · Electrospinning · GBR membrane

H.-. Zhang (✉) · J. Wang · N. Yu
College of Stomatology, Ningxia Medical University,
Yinchuan 750004, China
e-mail: hua31415926@163.com

J.-. Liu (✉)
Department of Prosthodontics, School and Hospital of Stomatology,
Wenzhou Medical University, Wenzhou 325027, China
e-mail: cecily5178@163.com

Introduction

The technique of dental implantation has become a common method of restoring missing teeth. However, due to the physiological absorption of bone after tooth loss or trauma-induced bone defects, 40–80 % of patients do not have enough bone to facilitate implantation surgery. In this situation, side perforation often occurs during the process of surgery, ultimately leading to implantation failure. However, the technique of guided bone regeneration (GBR), as proposed by Nyman et al. in the early 1980s, has been employed with some success to solve this problem [1]. The GBR technique is regarded as one of the most important methods for increasing the amount of bone in the alveolar ridge, which is often recommended for dental implantation surgery. In this technique, the GBR barrier membrane plays a very important role during the process of guided bone regeneration. This barrier membrane is placed on the bone dust such that it covers the bone defect area. It is a biological barrier which creates an isolated space that prevents the migration of gingival connective tissue cells and epithelial cells into the bone defect area, allows osteoblasts preferential access to this area, protects blood clots, and facilitates the generation of new bone.

Absorbable collagen membranes are increasingly being used as barrier membranes in clinical applications due to their superior properties. They are more stable but also more expensive. However, the main drawback of absorbable collagen membranes that they have relatively poor mechanical strength to maintain the isolated space compared to non-absorbable membranes. Therefore, it is necessary to develop a moderately priced absorbable membrane with good mechanical properties and cytocompatibility, resistance to infection, and excellent biocompatibility.

A single material is generally unable to meet these requirements. Therefore, much of the interest from researchers in this field has focused on creating composites made from combinations of different types of materials. Composite biomaterials

with a variety of excellent properties can be obtained by changing the composition of and the ratio of the components in the composite, as well as the interface between the different components. The most commonly employed combinations of composite materials include synthetic and natural materials or organic and inorganic materials. As well as such binary composites, those with more than two components could be used. Therefore, in the study reported in the present paper, we attempted to fabricate a composite GBR membrane for biomedical applications that has three components: a synthetic material, a natural material, and an inorganic material.

Poly(lactic-*co*-glycolic acid) (PLGA), a copolymer composed of PLA and PGA, is a biodegradable synthetic polymer. PLGA, which has been approved by the U.S. FDA, has been widely used for biomedical applications, including orthopedic fixation materials, surgical sutures, tissue regeneration materials, and carriers for drug and gene delivery. However, PLGA is not very hydrophilic so cell adhesion is weak, and it can also cause aseptic inflammation. Besides, cast PLGA films are mechanically brittle and thus unsuitable for use as GTR scaffolds.

Carbon nanotubes (CNTs), which exist as either single-walled carbon nanotubes (SWNTs) or multi-walled carbon nanotubes (MWNTs), are allotropes of carbon. They are considered to be typical one-dimensional nanomaterials. The unique carbon nanotube structure imbues carbon nanotubes with a number of special physical and chemical properties. The C=C covalent bond that is used to form carbon nanotubes is the most stable chemical bond in the natural world, so carbon nanotubes have excellent mechanical properties. They are considered to be ideal fillers for reinforcement purposes. It is also reported that the incorporation of even small quantities of CNTs into polymeric materials significantly improves their mechanical, optical, electrical, and thermal properties, and even their biocompatibilities [2–5].

Keratin is the main component of wool, feathers, nails, horns, and other epithelial coverings. The keratin content of wool is more than 50 wt%. Wool keratin, just like collagen, is a biological polymer consisting of polypeptide chains formed by the condensation of various amino acids, especially those containing many hydrophilic amino acids [6]. It is reported that wool keratin membranes are nontoxic, biodegrade within a specific timescale both *in vitro* and *in vivo* without causing inflammatory and immune responses, and are permit the attachment, differentiation, and proliferation of fibroblast cells and osteoblasts [7–9], suggesting that wool keratin could prove very useful for biomedical applications, in a similar manner to collagen. Moreover, compared to other proteins, wool keratin is readily available and costs less to extract, meaning that it possesses great potential as a source of protein and amino acids for biomedical applications [10, 11].

Therefore, in the present study, in an attempt to fabricate materials that better fulfill the requirements of an ideal GBR membrane, a synthetic material (PLGA), an inorganic

component (MWNTs), and a natural ingredient (wool keratin) were combined to create PLGA/MWNTs/wool keratin composite membranes by electrospinning. Electrospinning is a simple and efficient method for the production of nanofibers from both natural and synthetic materials that produces fibers with diameters in the micrometer to nanometer range [12, 13]. Electrospun membranes offer porosities and surface areas that resemble natural extracellular matrix and promote cell attachment, proliferation, and differentiation [5]. The morphological, mechanical, and thermal properties of the electrospun membranes and their bioactivities *in vitro* were observed. This study will provide the foundation for further studies on PLGA/MWNTs/wool keratin membranes for GBR applications.

Experimental

Materials

PLGA (M_w : 1×10^5 g/mol), with a lactide/glycolide ratio of 75:25 w/w, was purchased from Shandong Daigang Co., Ltd. (Jinan, China). MWNTs-COOH with diameters of 8–25 nm, lengths of 0.5–2 mm, and purities of >95 wt%, were purchased from Chengdu Organic Chemistry Co. Ltd. (Chengdu, China). The wool was purchased from Kunshan Sanli Wool Carbonization Co., Ltd. (Jiangsu, China). The wool keratin was extracted from clean wool according to previously published protocols [7]. In brief, keratin was extracted by incubation in an aqueous solution of urea, mercaptoethanol, and sodium dodecyl sulfate at 60 °C for 5 h. The solution containing wool keratin was then dialyzed for 4 days and spray-dried to obtain wool keratin powders. Dimethyl formamide (DMF), trichloromethane (TCM), and other analytical reagents were purchased from Tianjin Chemical Reagent Co., Ltd. (Tianjin, China).

Electrospinning of PLGA/MWNTs/wool keratin membranes

A 15-wt% PLGA solution was prepared by dissolving PLGA in a mixture of TCM and DMF (7:3 v/v). The MWNTs-COOH (0.5 wt%) and wool keratin (at four different levels: 0 wt%, 0.5 wt%, 1 wt%, or 2 wt%) were added to the PLGA solution. The solutions were sonicated for 1 h in order to accelerate the homogeneous dispersion of MWNTs and wool keratin. A grounded rotating drum (10 cm in diameter) covered with a piece of aluminum foil (10×10 cm²) was used to collect the fibers. It rotated at 4 m/min along the track. The blend solutions were loaded into a 5-mL plastic syringe with a blunt 18-gauge needle attached, and delivered via a syringe pump to control the flow rate (0.3 mL/min). The syringe pump was connected to a moving device that could move in both directions equidistantly along a straight line that is through the center. The speed and amplitude were set at 30 cm/min and 2 cm, respectively. The needle was pointed toward the aluminum foil,

and a constant positive voltage (15 kV) was applied to the needle. The distance between the needle tip and the collecting drum was 16 cm. All electrospinning experiments were carried out at room temperature.

Instrumental characterization of the PLGA/MWNTs/wool keratin membranes

The surface morphologies of the electrospun fibers were observed using a JSM-5900LV scanning electron microscope (SEM; JEOL, Tokyo, Japan) at 20 kV. The average diameter of the electrospun fibers was determined by SEM by analyzing 50 single fibers using the Sigma Scan Pro 2.0 software (Systat Software, Inc., Chicago, IL, USA). The samples for transmission electron microscopy (TEM, JEM-100CX, JEOL, Japan) were prepared by directly depositing the fibers onto the copper grids. The TGA thermograms of the fibers were analyzed with a thermogravimetric analyzer (TAQ600; TA Instruments, New Castle, DE, USA) in a nitrogen atmosphere. The temperature was increased from room temperature to 400 °C at 10 °C/min. The weight of each specimen was maintained at ~5 mg. Tensile testing was performed on the fibrous membranes using a universal testing machine (Instron 5567; TestResources, Inc., Shakopee, MN, USA) at room temperature. Samples were stretched to failure at a rate of 5 mm/min, and the load cell used was 100 N with a gauge length of 25 mm. The dimensions of the samples used were 1 cm×7 cm×100–150 μm. The tensile test was repeated six times per sample.

Assessment of bioactivity in 1.5×simulated body fluid (SBF)

The method of biomimetic mineralization (reported previously) was used to assess the bioactivities of the PLGA/MWNTs/wool keratin membranes. 1.5×SBF was prepared based on an established protocol developed by Varma [14]. Briefly, NaCl, KCl, CaCl₂, MgCl₂·6H₂O, NaHCO₃, K₂HPO₄·3H₂O, and Na₂SO₄ were dissolved in deionized water. The pH value of the solution was adjusted with HCl, and the final pH of the solution was 7.3. The ion concentrations in the 1.5×SBF were 213.0 mM Na⁺, 3.8 mM Ca²⁺, 2.3 mM Mg²⁺, 7.5 mM K⁺, 221.9 mM Cl⁻, 1.5 mM HPO₄²⁻, 6.3 mM HCO₃⁻, and 0.7 mM SO₄²⁻. The PLGA/MWNTs/2.0 % wool keratin membranes (20 mm×20 mm) were soaked in a freshly prepared saturated Ca(OH)₂ solution at room temperature for 1 h at first, and then rinsed with distilled water. Subsequently, the membranes were immersed in 1.5×SBF at 37 °C for 7 or 14 days. The 1.5×SBF was replaced every 24 h. At the end of the incubation time, the samples were rinsed with deionized water and then dried under vacuum at room temperature. The morphologies of the samples were observed with SEM (JSM-5900LV, JEOL, Tokyo, Japan) at an accelerating voltage of 20 kV. Elemental analysis of the crystals was by EDS (JSM-7500 F, JEOL). An X-ray diffractometer (SA-HF3, Rigaku,

Tokyo, Japan) was used to investigate the mineral crystals grown on the surfaces of the membranes. XRD was carried out with a Ni-filtered CuKα radiation source operated at a voltage of 40 kV and a current of 30 mA. The samples were scanned from 3 to 80° (2θ) and the scan rate was 8°/min.

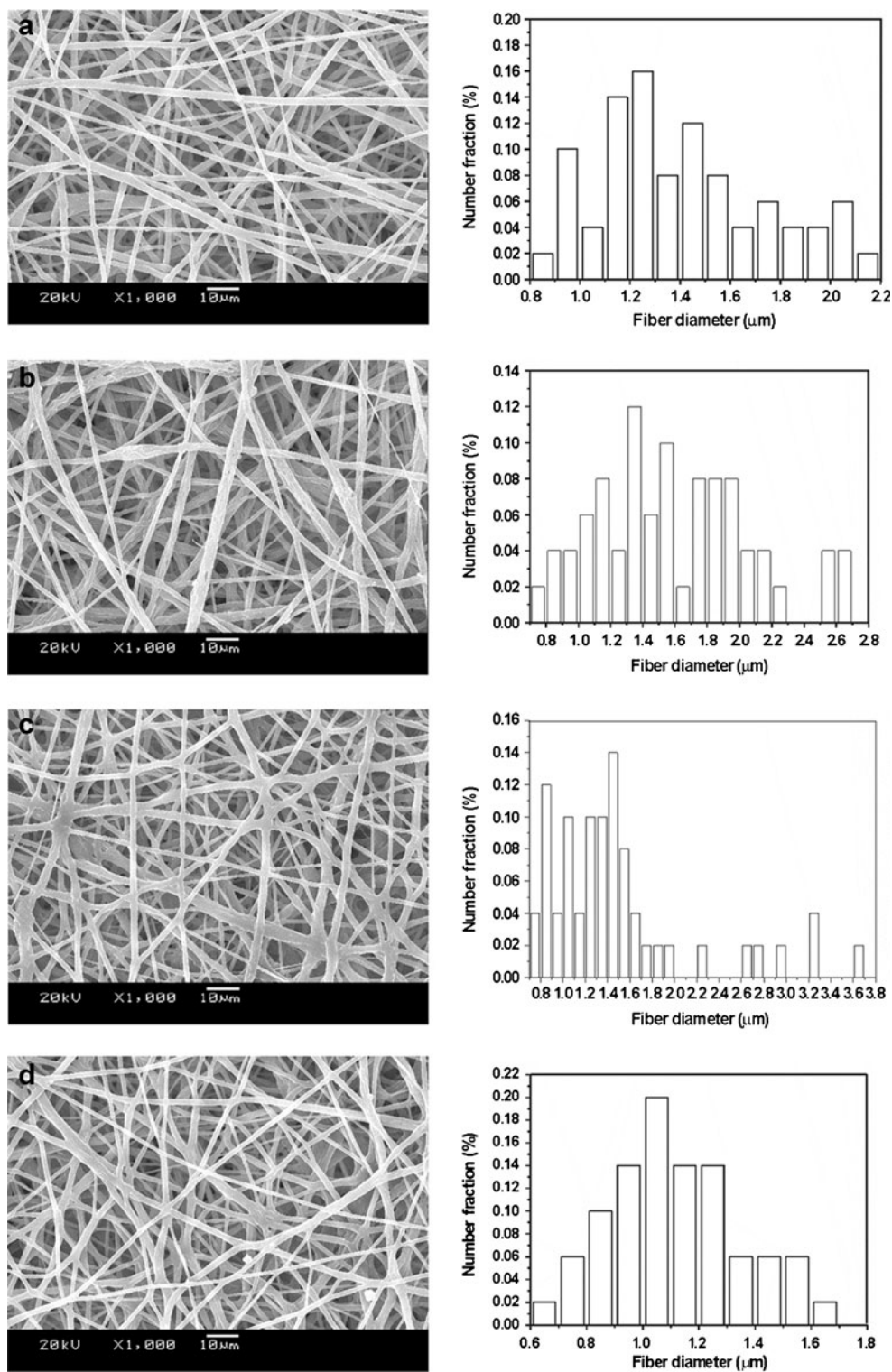
Results and discussion

Morphological characterization of electrospun PLGA/MWNTs/wool keratin fibers

Figure 1 shows SEM images and the corresponding fiber diameter distributions of the electrospun composite fibers with various concentrations of wool keratin (ranging from 0 to 2.0 wt%). As shown in Fig. 1a, the electrospun PLGA/MWNTs fibers exhibited smooth outer surfaces and randomly oriented and long, fibrous morphologies, indicating that the MWNTs were effectively dispersed in the PLGA/MWNTs composite fibers. The diameters ranged from 800 to 2200 nm, with an average of about 1411 nm. When 0.5 wt% wool keratin was added to the PLGA/MWNTs solution, the PLGA/MWNTs/0.5 % wool keratin fibers became more curved, and many wrinkles appeared on the surfaces of the fibers. In addition, the fiber diameters were thicker and had a broader range of diameters (700–2700 nm), with an average diameter of about 1595 nm. As the content of wool keratin was increased further, the morphologies of the composite fibers (Fig. 1c and d) were observed to be similar to that of PLGA/MWNTs/0.5 % wool keratin fibers, with many wrinkles on the fiber surface. The PLGA/MWNTs/1.0 % wool keratin fibers had a broader range of diameters (700–3700 nm; average 1403 nm), while the majority of the PLGA/MWNTs/2.0 % wool keratin fibers had diameters of 600–1700 nm (average 1128 nm). The PLGA/MWNTs/2.0 % wool keratin fibers were the thinnest. It was observed that the average diameter of the PLGA/MWNTs/wool keratin fibers initially increased and then decreased as the wool keratin content was increased from 0.5 to 2 %. Differences in fiber diameter were likely due to differences in the conductivities and viscosities of the electrospun solutions [15].

Figure 2 shows TEM images of the MWNTs, the electrospun PLGA fibers, and the PLGA/MWNTs/2.0 % wool keratin composite fibers. It is clear that the surfaces of the PLGA fibers were smooth and uniform, while those of the PLGA/MWNTs/2.0 % wool keratin fibers became rougher and some of the wool keratin particles were partially exposed on the surfaces of fibers. However, most of the wool keratin particles were well dispersed and encapsulated within the fibers, and some of the particles tended to agglomerate and were even observed to protrude from the outer surface layers of the composite fibers. Figure 2d shows that the MWNTs are embedded and well dispersed in the composite fibers and

Fig. 1 SEM images and the corresponding fiber diameter distributions of the electrospun PLGA/MWNTs (a), PLGA/MWNTs/0.5 % WK (b), PLGA/MWNTs/1.0 % WK (c), and PLGA/MWNTs/2.0 % WK (d) membranes (WK: wool keratin)



aligned along the fiber axis, indicating that good alignment of MWNTs was achieved in the composite fibers during the electrospinning process. It can be deduced that the application of high electrostatic fields during the electrospinning process would be expected to result in MWNT orientation along the fiber axis [16].

Mechanical properties of electrospun PLGA/MWNTs/wool keratin fibers

Figure 3 shows the tensile stress–strain curves of the PLGA, PLGA/MWNTs, and the series of PLGA/MWNTs/wool keratin membranes. The associated data are summarized in

Fig. 2 TEM images of electrospun PLGA fibers (a), PLGA/MWNTs/2.0 % WK fibers (b, d), and MWNTs (c)

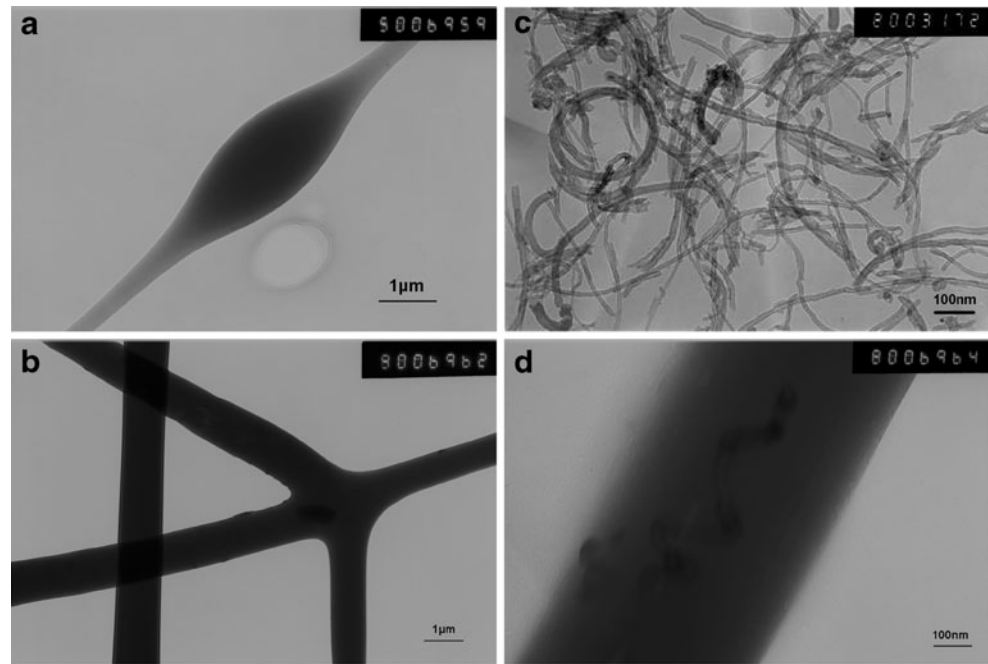


Table 1. As can be seen from Fig. 3, the mechanical properties of the PLGA/MWNTs and PLGA/MWNTs/wool keratin membranes were significantly different from those of the pure PLGA fibers. Results showed that the pure PLGA film was somewhat fragile, judging by its low ultimate strength and elongation at break. Compared to the pure PLGA membrane, the ultimate strength of the PLGA/MWNTs membrane was 42 % higher (increasing from 5.60 to 7.98 MPa); its Young's modulus was 9 % higher (increasing from 307.12 to 334.61 MPa); and its elongation at break was 388 % higher (increasing from 14.35 % to 70.07 %). It is obvious that the incorporation of the MWNTs had a profound effect on the tensile properties of the composites, and that the introduction of even a small amount of MWNTs significantly improved the tensile strength of the composites [17–20]. This could be due to the higher crystallinity and higher degree of orientation of the molecular chains of the composite fibers with 0.5 wt% MWNTs [17]. When the level of wool keratin was increased from 0 % to 0.5 %, the elongation at break increased, but the ultimate strength and Young's modulus decreased a little, indicating that the PLGA/MWNTs/0.5 % wool keratin fibers were softer. However, as the content of wool keratin in the composites was further increased to 2.0 %, the ultimate strength, elongation at break, and Young's modulus reached their highest levels; that is, 13.93 Mpa, 104.02 %, and 824.30 MPa, respectively. The improved ultimate strength and Young's modulus values of the composites fibers indicated that the composites were tougher and more resistant to deformation. This may be due to the interaction between the homogeneously dispersed wool keratin, the MWNTs, and the polymer chains [17].

Thermal stability of electrospun PLGA/MWNTs/wool keratin fibers

Thermal analysis was conducted to evaluate the thermal stabilities of the electrospun membranes. Figure 4 compares the TGA and derivative thermogravimetric (DTG) diagrams for the composites. The initial decomposition temperatures at weight losses of 10 %, 20 %, 60 %, and 90 % (T10 %, T20 %, T60 %, and T90 %, respectively) are summarized in Table 2. Single-step degradation was observed in all samples. The initial weight loss of PLGA fibers took place at 100–225 °C, which was due to moisture loss. The second weight loss took place in the temperature range 225–300 °C, and was due to the thermal degradation of the PLGA matrix. However, the PLGA/MWNTs and PLGA/MWNTs/wool keratin films showed higher thermal stabilities than the pure PLGA

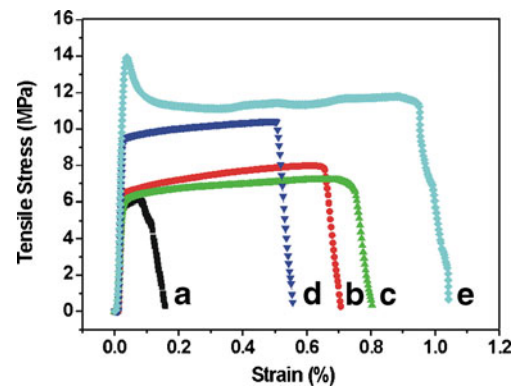


Fig. 3 The tensile stress–strain curves of the electrospun PLGA membrane (a) and the PLGA/MWNTs (b), PLGA/MWNTs/0.5 % WK (c), PLGA/MWNTs/1.0 % WK (d) and PLGA/MWNTs/2.0 % WK (e) composite membranes

Table 1 Mechanical properties of the PLGA membrane and the PLGA/MWNTs and PLGA/MWNTs/wool keratin composite membranes

Sample	Ultimate strength (Mpa)	Elongation at break (%)	Young's modulus (Mpa)
PLGA	5.60	14.35	307.12
PLGA/MWNTs	7.98	70.07	334.61
PLGA/MWNTs/ 0.5 % wool keratin	7.19	79.40	234.11
PLGA/MWNTs/ 1.0 % wool keratin	10.44	53.45	651.84
PLGA/MWNTs/ 2.0 % wool keratin	13.93	104.02	824.30

membrane. Their initial weight losses took place at about 100–300 °C, and the second weight losses took place in the temperature range 300–350 °C. As shown in Table 2, the T10 %, T20 %, T60 %, and T90 % values of the PLGA/MWNT film were all higher than those of the pure PLGA membranes by 20–40 °C, highlighting the excellent thermal and thermo-oxidative stabilities of PLGA/MWNTs composites. This demonstrates that even a small amount of MWNTs can provide effective reinforcement against thermal degradation of the polymer matrix, increasing the thermal stability of the matrix. The maximum thermal degradation temperatures were 286.39 °C, 317.58 °C, 318.38 °C, 318.92 °C, and 318.90 °C, respectively (Fig. 4b), whereas the decomposition temperatures of the PLGA/MWNTs/wool

Table 2 Thermal stabilities of the PLGA membrane and the PLGA/MWNTs and PLGA/MWNTs/wool keratin composites

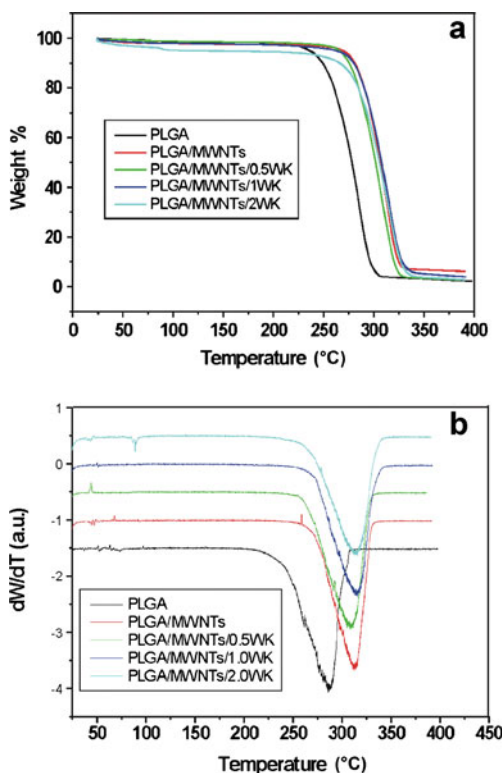
Sample	T10 °C	T20 %	T60 %	T90 %
PLGA	248.87	273.18	282.43	296.23
PLGA/MWNTs	287.32	296.88	316.26	330.70
PLGA/MWNTs/0.5 % WK	286.10	295.59	316.39	330.54
PLGA/MWNTs/1.0 % WK	285.37	295.85	317.35	333.61
PLGA/MWNTs/2.0 % WK	272.60	291.00	316.74	333.11

keratin fibers were at least as high as those of the PLGA/MWNTs fibers, and gradually increased with wool keratin content. These results are consistent with the results obtained from the TGA experiments (Fig. 4a and Table 2). The thermal stabilities of the PLGA/MWNTs/wool keratin fibers were similar to that of the PLGA/MWNTs scaffold. This may be attributed to the high crystallinity of the β -sheet structure in wool keratin, in which there are strong intermolecular interactions between the protein chains [21].

Bioactivities of the PLGA/MWNTs/wool keratin membranes

The morphologies of the PLGA/MWNTs/2.0 % wool keratin membranes after incubation in SBF for 7 and 14 days were evaluated using SEM. Small spherical and hemispherical mineral crystals were deposited randomly on the surfaces of the PLGA/MWNTs/wool keratin fibers after incubation in $1.5\times$ SBF for 7 days at 37 °C (Fig. 5a). After 14 days of incubation, the number of mineral crystals on the PLGA/MWNTs/wool keratin fibers had increased significantly, and the mineral layers completely covered the surfaces of the fibers (Fig. 5b). Even viewing with the naked eye, it was apparent that the surfaces of the samples were covered with layers of white mineralized crystals. However, the $1.5\times$ SBF remained clear, indicating that heterogeneous nucleation occurred on the surfaces of the composite membranes [22, 23]. In higher magnification images (Fig. 5c), it can be seen that the crystals were nanosized.

X-ray diffractograms of the PLGA/MWNTs/2.0 % wool keratin membranes and the samples immersed in $1.5\times$ SBF for 7 days and 14 days are shown in Fig. 6. After 7 days of incubation, weak and wide diffraction peaks at $2\theta=26^\circ$, 32° , and 54° appeared, which were consistent with the main characteristic diffraction peaks of the hydroxyapatite (HA) compared with the JCPDS standard card of HA, and these peaks corresponded to planes (002), (211), and (004) of HA, respectively. When the incubation time was increased to 14 days, the diffraction peaks at $2\theta=26^\circ$, 32° , and 54° all grew stronger and narrower, indicating that the amount and the size of the apatite crystals increased, and the crystallinity also improved with increasing immersion time [24]. However, diffraction peaks were not observed for the other planes of HA. This is because the mineral crystals on the films have a preferred

**Fig. 4** TGA curves (a) and derivative thermogravimetric (DTG) curves (b) for the composites

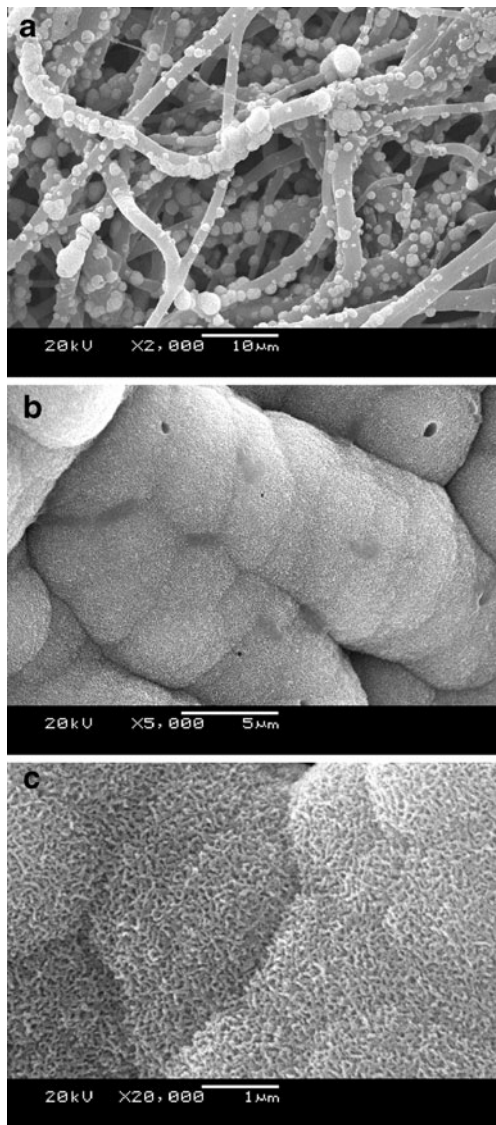


Fig. 5 SEM images of the PLGA/MWNTs/2.0 % WK membranes after immersion in 1.5×SBF for **a** 7 days and **b, c** 14 days

orientation for nucleation and growth. The mineral crystals grow along a certain axial direction, causing some planes to overlap and some diffraction peaks to disappear due to crystal growth defects [25].

EDS was used to analyze the type and proportion of elements in the crystals. As shown in Table 3, the Ca/P molar ratios for the PLGA/MWNTs/2.0 % wool keratin membranes after 7 days and 14 days of incubation were 2.16 and 1.89, respectively, which were all slightly higher than that of the chemical dose HA (Ca/P =1.67). It can therefore be deduced that the phosphate in apatite crystals may be replaced by other groups.

Biomimetic mineralization is based on the principles of heterogeneous nucleation. In the biomineralized structures analyzed to date, the process of mineral deposition may be termed “matrix regulated.” First, after pre-functionalization, the substrate surface is immersed in a supersaturated biomimetic

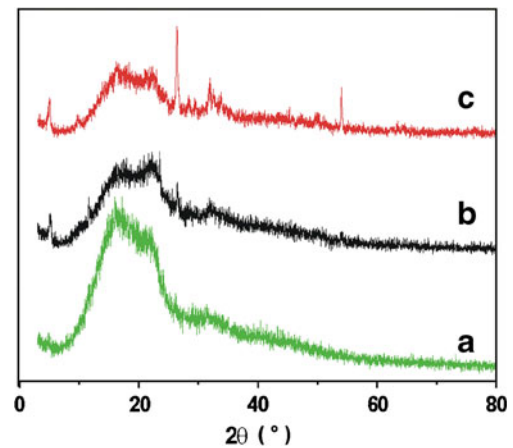


Fig. 6 XRD patterns of PLGA/MWNTs/2.0 % WK composite membranes (**a**) and PLGA/MWNTs/2.0 % WK composite membranes after immersion in 1.5×SBF for 7 days (**b**) and 14 days (**c**)

solution. When homogeneous precipitation cannot occur under the conditions of insufficient supersaturation, heterogeneous nucleation of crystals takes place on the substrate surface, and the crystals spontaneously grow into mineral layers. The processes of crystal nucleation and growth occur at different times and are regulated by complementary and redundant feedback control loops, which are crucial for countering the thermodynamic driving force that leads to unrestricted mineralization from a supersaturated environment [26].

The functional groups which can guide nucleation are Si–OH, –H₂PO₄, –COOH, –CONH₂, –OH, and so on. The common feature of these functional groups is that they are negatively charged at around pH7.40. These functional groups cannot directly induce nucleation during apatite mineralization; instead, they react with calcium ions to form compounds with calcium-containing functional groups, and then noncrystalline calcium phosphate forms with a low Ca/P ratio. As the mineralization is initiated by the compounds with calcium-containing functional groups, and there are chemical bonds between the matrix and the mineral crystals, the binding strength is higher than that of the mineral when it is deposited in the normal manner [27].

Conclusions

Nonwoven PLGA/MWNTs/wool keratin membranes intended for further GBR applications were successfully fabricated by electrospinning. The average diameter of the

Table 3 Ca/P molar ratio of apatite on the surfaces of PLGA/MWNTs/2.0 % wool keratin membranes after 7 days and 14 days of incubation

Incubation period	Ca/P ratio
7 days	2.16
14 days	1.89

PLGA/MWNTs/wool keratin fibers first increased and then decreased as the wool keratin content was increased from 0.5 % to 2 %. MWNTs and wool keratin particles were well dispersed throughout the PLGA matrix according to the results of TEM. Adding MWNTs and wool keratin to the PLGA composites increased the mechanical properties of the resulting PLGA/MWNTs/wool keratin composites. The ultimate strength, elongations at break, and Young's modulus values of the PLGA/MWNTs/2.0 % wool keratin composites reached their highest levels. All of the PLGA/MWNTs/wool keratin composites showed high thermal and thermooxidative stabilities. Apatite crystals of low crystallite size and crystallinity formed on the composite membranes after immersion in $1.5 \times$ SBF, suggesting that the PLGA/MWNTs/wool keratin composites are bioactive in vitro. These results suggest that the PLGA/MWNTs/wool keratin composites may be used as GBR membranes for bone tissue regeneration. However, further studies on their biocompatibility in vitro and in vivo and their degradability are needed.

Acknowledgments This study was supported by the National Natural Science Foundation of China (grant numbers 81200818, 81360269, and 81371182), the Key Project of the Ministry of Education of China (grant number 211196), and the Scientific Research Foundation for Higher Education of Ningxia Province of China (grant number NXY2012058).

References

- Nyman S, Lindhe J, Karring T, Rylander H (1982) New attachment following surgical treatment of human periodontal disease. *J Clin Periodontol* 9:290–296
- Saeed K, Park S-Y (2007) Preparation of multiwalled carbon nanotube/nylon-6 (MWNTs/nylon) nanocomposites by in-situ polymerization. *J Appl Polym Sci* 106:3729–3735
- Ayutsede J, Gandhi M, Sukigara S, Ye H, Hsu CM, Gogotsi Y, Ko F (2006) Carbon nanotube reinforced *Bombyx mori* silk nanofibers by the electrospinning process. *Biomacromolecules* 7:208–214
- Chen D, Liu TX, Zhou XP, Chauhari Tjiu WW, Hou HQ (2009) Electrospinning fabrication of high strength and toughness polyimide nanofiber membranes containing multiwalled carbon nanotubes. *J Phys Chem B* 113:9741–9748
- Zhang H (2011) Electrospun poly (lactic-co-glycolic acid)/multiwalled carbon nanotubes composite scaffolds for guided bone tissue regeneration. *J Bioact Compat Pol* 26:347–362
- Ki CS, Gang EH, Um IC, Park YH (2007) Nanofibrous membrane of wool keratose/silk fibroin blend for heavy metal ion adsorption. *J Membrane Sci* 302:20–26
- Yamauchi K, Yamauchi A, Kusunoki T, Kohda A, Konishi Y (1996) Preparation of stable aqueous solution of keratins, and physicochemical and biodegradational properties of films. *J Biomed Mater Res* 31: 439–444
- Yamauchi K, Mniwa M, Mori T (1998) Cultivation of fibroblast cells on keratin-coated substrata. *J Biomater Sci Polym Ed* 9:259–270
- Tanabe T, Okitsu N, Tachibana A, Yamauchi K (2002) Preparation and characterization of keratin-chitosan composite film. *Biomaterials* 23:817–825
- Yang X, Zhang H, Yuan XL, Cui SX (2009) Wool keratin: a novel building block for layer-by-layer self-assembly. *J Colloid Interf Sci* 336:756–760
- Gousterova A, Braikova D, Goshev I, Christov P, Tishinov K, Vasileva-Tonkova E, Haertlé T, Nedkov P (2005) Degradation of keratin and collagen containing wastes by newly isolated thermoactinomycetes or by alkaline hydrolysis. *Lett Appl Microbiol* 40:335–340
- Suwantong O, Pankongadisak P, Deachathai S, Supaphol P (2012) Electrospun poly(L-lactic acid) fiber mats containing a crude *Garcinia cowa* extract for wound dressing applications. *J Polym Res* 19:9896–9905
- Ma C, Huang DL, Chen HC, Chen DL, Xiong ZC (2012) Preparation and characterization of electrospun poly(lactide-co-glycolide) membrane with different L-lactide and D-lactide ratios. *J Polym Res* 19: 9803–9808
- Varma HK, Yokogawa Y, Espinosa FF, Kawamoto Y, Nishizawa K, Nagata F, Kameyama T (1999) Porous calcium phosphate coating over phosphorylated chitosan film by a biomimetic method. *Biomaterials* 20:879–884
- Zhang HL (2011) Effects of electrospinning parameters on morphology and diameter of electrospun PLGA/MWNTs fibers and cytocompatibility in vitro. *J Bioact Compat Pol* 26:590–606
- Wei K, Xia JH, Kim BS, Kim IS (2011) Multiwalled carbon nanotubes incorporated *Bombyx mori* silk nanofibers by electrospinning. *J Polym Res* 18:579–585
- Saligheh O, Forouharshad M, Arasteh R, Eslami-Farsani R, Khajavi R, Yadollah Roudbari B (2013) The effect of multiwalled carbon nanotubes on morphology, crystallinity and mechanical properties of PBT/MWCNT composite nanofibers. *J Polym Res* 20:65–70
- Volpato FZ, Ramos SLF, Motta A, Migliaresi C (2011) Physical and in vitro biological evaluation of a PA 6/MWCNT electrospun composite for biomedical applications. *J Bioact Compat Polym* 26:35–47
- Han CT, Chi M, Zheng YY, Jiang LX, Xiong CD, Zhang LF (2013) Mechanical properties and bioactivity of high-performance poly(etheretherketone)/carbon nanotubes/bioactive glass biomaterials. *J Polym Res* 20:203–210
- Lin CL, Wang YF, Lai YQ, Yang W, Jiao F, Zhang HG, Ye S, Zhang Q (2011) Incorporation of carboxylation multiwalled carbon nanotubes into biodegradable poly(lactic-co-glycolic acid) for bone tissue engineering. *Colloids Surf B Biointerfaces* 83:367–375
- Um IC, Kweon HY, Park YH, Hudson S (2001) Structural characteristics and properties of the regenerated silk fibroin prepared from formic acid. *Int J Biol Macromol* 29:91–97
- Jakobsen RJ, Brown LL, Hutson TB, Fink DJ, Veis A (1983) Intermolecular interactions in collagen self assembly as revealed by Fourier transform infrared spectroscopy. *Science* 220:1288–1290
- Linde A (1995) Dentin mineralization and the role of odontoblasts in calcium transport. *Connect Tissue Res* 33:163–170
- Zhang HL, Liu JS, Yao ZW, Yang J, Pan LZ, Chen ZQ (2009) Biomimetic mineralization of electrospun poly(lactic-co-glycolic acid)/multi-walled carbon nanotubes composite scaffolds in vitro. *Mater Lett* 63:2313–2316
- Varma HK, Yokogawa Y, Espinosa FF, Kawamoto Y, Nishizawa K, Nagata F, Kameyama T (1999) In-vitro calcium phosphate growth over functionalized cotton fibers. *J Mater Sci Mater Med* 10:395–400
- Heuer AH, Fink DJ, Laraia VJ, Arias JL, Calvert PD, Kendall K, Messing GL, Blackwell J, Rieke PC, Thompson DH (1992) Innovative materials processing strategies: a biomimetic approach. *Science* 255:1098–1105
- Kokubo T, Kim HM, Kawashita M, Nakamura T (2001) Process of calcification on artificial materials. *Z Kardiol* 90(Suppl 3):86–91